Malaysian Journal of Analytical Sciences (MJAS)
Published by Malaysian Analytical Sciences Society

CONSTRUCTING NI-DOPED ZnO/GO HETEROSTUCTURES FOR ENHANCED SUNLIGHT-TRIGGERED DEGRADATION OF METHYLENE BLUE DYE

(Pembinaan Heterostruktur Ni-Didop dengan ZnO/GO untuk Meningkatkan Degradasi Pewarna Metilina Biru di Bawah Sinar Matahari)

Hartini Ahmad Rafaie[1,5]*, Nur Shafiza Ismail[1], Syazni Hanun Nur Ili Dedy Dasiano[2,4], Muhd Firdaus Kasim[3], Nurul Infaza Talalah Ramli[1], Zul Adlan Mohd Hir[1], Mohomad Hafiz Mamat[4]

[1]Faculty of Applied Science,
Universiti Teknologi MARA Pahang, 26400 Bandar Tun Abdul Razak Jengka, Pahang, Malaysia
[2]Faculty of Applied Sciences
[3]Center for Nanomaterials Research, Institute of Science
[4]NANO-Electronic Centre, Faculty of Electrical Engineering
Universiti Teknologi MARA, 40450 Shah Alam, Selangor, Malaysia
[5]Centre of Foundation Studies,
Universiti Teknologi MARA, Selangor Branch, Dengkil Campus, 43800 Dengkil, Selangor, Malaysia

**Corresponding author: hartinirafaie@uitm.edu.my*

Received: 15 November 2021 ; Accepted: 3 February 2022 ; Published: 27 June 2022

Abstract

Chemical pollutants emitted by the textile industry are a major source of water contamination, resulting in dangerous diseases and most of the effluent treatment techniques are relatively ineffective. As a result, metal oxide-based photocatalysts emerged as a viable alternative to the already existing dye treatment methods. The current work focused on the synthesis and characterization of Ni-doped ZnO/GO heterostructures and evaluation of its photoactivity under sunlight irradiation. The nanocomposite was prepared via a simple mixing approach, by varying the weight ratio of graphene oxide (GO) ranging from 0.1 to 0.4 g prior to the incorporation into Ni-doped ZnO surfaces. The X-ray diffraction analysis revealed that Ni and GO were successfully incorporated into the wurtzite-structure of ZnO nanocomposites. FESEM images showed a uniformed particle with the average size of about 100-500 nm for all samples. The photocatalytic activity was assessed by monitoring the degradation of methylene blue (MB) dye under direct sunlight irradiation. Ni-doped ZnO/$GO_{0.1}$ nanocomposite exhibited the greatest degradation performance by degrading 94% MB. The highest degradation rate constant of 0.0250 min^{-1} was obtained within 120 minutes of reaction time. The current study is easy, effective, and compatible; hence it can be employed in the future to treat textile dye wastewater.

Keywords: graphene oxide, methylene blue, nickel, photodegradation, sunlight

Abstrak

Bahan pencemar kimia yang dikeluarkan oleh industri tekstil merupakan sumber utama pencemaran air, mengakibatkan penyakit berbahaya dan kebanyakan kaedah rawatan sisa bahan buangan yang dicipta masih tidak berkesan sepenuhnya. Justeru,

fotomangkin berasaskan logam oksida dihasilkan sebagai alternatif yang berdaya maju bagi kaedah rawatan pewarna sedia ada. Penumpuan kepada sintesis dan pencirian yang mudah bagi heterostruktur ZnO/GO yang didopkan dengan Ni dan penilaian fotoaktivitinya di bawah cahaya matahari. Nanokomposit disediakan melalui kaedah campuran yang ringkas dengan mengubah nisbah berat grafin oksida (GO) diantara 0.1 hingga 0.4 g sebelum dimasukkan ke dalam permukaan ZnO berdop Ni. Analisis pembelauan sinar-X mendedahkan bahawa Ni dan GO telah berjaya dimasukkan ke dalam struktur ZnO. Imej FESEM menunjukkan partikel seragam dengan saiz purata diantara 100-500 nm untuk semua sampel. Aktiviti fotokatalitik dinilai dengan memantau degradasi pewarna metilina biru (MB) di bawah penyinaran cahaya matahari secara lansung. Nanokomposit $ZnO/GO_{0.1}$ berdop Ni mempamerkan prestasi degradasi yang paling tinggi dengan nilai peratus degradasi 94% MB. Pemalar kadar degradasi tertinggi ialah 0.0250 min^{-1} diperolehi dalam masa 120 minit masa tindak balas. Kajian ini didapati mudah, berkesan dan sesuai, justeru ia boleh digunakan pada masa hadapan untuk merawat sisa buangan pewarna dari industri tekstil.

Kata kunci: grafin oksida, metilina biru, nikel, fotodegradasi, cahaya matahari

Introduction

In the past decades, contamination of freshwater resources with a large amount of dyes has been widely reported, mainly due to the rapid industrialization. They are employed in textile, paper, foods, cosmetics, pharmaceuticals, and printing industries [1]. The dyes are believed to have found their way entering the groundwater through dyeing process, leaching from various dye industries, and inappropriate discharge of untreated dye effluents [2, 3]. Human exposures to dyes occurred through consumption of food, water, air inhalation and direct contact with body and skin. This exposures hence have affected the human health and aquatic lives due to their toxicity [4, 5]. It is therefore essential to use promising treatment strategies, aiming to restore the quality of contaminated water by ensuring the sustainability of the environments with economically viable approach.

Presently, photocatalytic advanced oxidation processes (AOPs) have been studied extensively for water restoration, mainly due to its favorable degradation activity toward recalcitrant organic pollutants as compared to conventional water treatment approaches [6, 7]. The method highlights on the use of semiconductor oxides as the catalyst assisted with UV or solar irradiation during the process. It is a cost-effective method in such a way that it operates at/near ambient temperature and pressure for the *in-situ* production of reactive radical species such as •OH and $•O_2^-$ on the surface of the photocatalyst [8]. The process aims for the mineralization of the contaminants to harmless inorganic by-products, water, and carbon dioxide through a series of redox reaction [9]. Of various semiconductor metal oxides, zinc oxide (ZnO) is most likely to be of the highest interest and regarded as an ideal catalyst due to its exceptional capability such as wide and direct bandgap semiconductor materials, higher photocatalytic efficiency, ability to absorb over a larger fraction of the UV or solar spectrum, non-toxic, low cost and environmentally sustainable [10–13].

Nonetheless, ZnO has their own limitation such as lower reusability and adsorption ability, wide band gap energy (3.37 eV) which can only be fully utilized under UV ($\lambda < 387$ nm) [14]. It is well-established that solar light consists of merely ~4% UV, so it is not very effective for large band gap materials. Also, rapid charge recombination is believed to be a major loss for the photoexcited charge carriers and a critical factor that limits the photo-efficiency for wide band gap photocatalyst [15–17]. To overcome these drawbacks, the construction of heterojunctions by coupling ZnO with suitable band potentials materials has been revealed to be an efficient strategy to simultaneously improve its photoactivity and photostability. Researchers found that modifying ZnO surface by doping with metal such as nickel (Ni) could extend the light absorption range towards visible region [18]. In this respect, Tawale et al. [19] investigated different microstructural and photoluminescence performance of bare ZnO, Ni doped ZnO and Cr doped ZnO. The result revealed that the Ni-doped ZnO nanostructures had the stronger PL intensity compared to Cr doped and undoped ZnO nanostructures. Apparently, high quality and good physicochemical properties will enhance the photocatalytic properties.

Wang et al. [18] reported on the recyclable photocatalyst based on flower-like nickel zinc ferrite nanoparticles/ZnO (NZF/ZnO) using a hydrothermal method. It was found that the samples prepared using 2.0 wt.%, 4.0 wt.% and 6.0 wt.% NZF nanoparticles exhibit better degradation performance towards rhodamine B (RhB) with increasing amounts of NZF, and 6.0 wt.% NZF has the best photocatalytic activity under visible irradiation. This result may come from the fact that the sample grown with 6.0 wt.% NZF has a smaller diameter and a larger surface area. Moreover, the much higher photocatalytic performance comes from the charge separation effect due to the band alignment between NZF and ZnO.

Combination of semiconductor oxide on carbonaceous materials such as graphene oxide is also attractive to improve the charge separation efficiency for enhanced photoactivity. This is due to the fascinating properties of GO such as high adsorption capacity, high electron mobility, large surface area and high thermal conductivity [4, 20–23]. This can be seen from the research conducted by Wu and Wang [24], where they conducted a study on the preparation of graphene oxide/hexagonal flower-like ZnO (GO/ZnO) micro/nanoparticles through hydrothermal method. It was found that the degradation percentage of rhodamine (RhB) dye reached 90.8% in 60 min, which was much higher than pure ZnO. The micro/nanostructure of GO/ZnO significantly improved the photocatalytic ability compared to pure ZnO. Kherabadi and his co-workers [4] reported on the synthesis, physicochemical properties and performance of three-dimensional (3D) Ag/ZnO/graphene as photocatalyst using a combined hydrothermal-photo deposition method. The dye degradation under both UV and visible light irradiation exhibited an enhanced photoactivity in comparison to ZnO/graphene and graphene alone. The deposition of Ag nanoparticles onto the surface of ZnO/graphene enhanced the photocatalytic efficiency due to the electron capturing properties.

In this research, an attempt has been made to synthesize Ni-doped ZnO/GO nanocomposites using a simple mixing approach. The morphological, structural properties, and photocatalytic activities of the nanocomposites were also investigated utilizing methylene blue (MB) dye as the probe molecule. Attempts has made to investigate the influence of variation GO weight ratio to Ni-doped ZnO on its performance as photocatalyst. The resultant nanocomposite photocatalyst certainly tends to harvest direct sunlight absorption effectively for photoexcited electron-holes formation, enhance the interfacial charge migration and hold better photostability during the photocatalytic reaction. The growth of Ni-doped ZnO/GO provides a simple, environmentally friendly and cost saving approach.

Materials and Methods

Materials

Commercial zinc oxide powder (ZnO, purity > 99%), Graphene oxide powder (GO, purity > 99%), nickel powder (Ni, purity > 99%), and methylene blue dye were purchased from Merck (Selangor, Malaysia). All chemicals and reagents were used as received and no purification step was performed. Deionized water was utilized throughout the synthesis and other experimental process.

Synthesis of Ni-doped ZnO/GO nanocomposites

In this work, a simple mixing approach was employed to prepare the heterostructures photocatalyst. Firstly, 0.5 g of Ni and 9.5 g of ZnO powder were mixed in a 100 mL of deionized water under continuous magnetic stirring for 30 min. After that, GO was added into the mixture and the amount was varied from 0.1 to 0.4 g. The amount of Ni and ZnO powder was kept constant throughout the process. The mixed solution went through an ultrasonic agitation using a sonicator (Powersonic 405) at a power of 350 W with a 40 KHz working frequency for 60 min. Following that, the mixtures solution was continuously stirred with a heating temperature of 60°C for 1 h on magnetic stirrer. Subsequently, the obtained Ni-doped ZnO/GO catalysts in the form of a fine powder were filtered, washed several times with deionized water and dried at 300°C for 1 h, yielding a greyish powder. The samples were labelled as ZnO/Ni, ZnO/Ni/$GO_{0.1}$, ZnO/Ni/$GO_{0.2}$, ZnO/Ni/$GO_{0.3}$, and ZnO/Ni/$GO_{0.4}$ accordingly. The morphology of the Ni-doped ZnO/GO nanocomposites was examined using a field emission scanning electron

microscopy (JEOL JSM-7600F). X-ray diffraction patterns were obtained by PANalytical X'pert Pro powder diffraction equipment at room temperature (Cu Kα radiations of λ =1.5418 Å) between 2θ range of 10–90° with a scanning speed of 2°/min. Following that, the Ni-doped ZnO/GO samples then underwent photocatalytic degradation measurement.

Photocatalytic degradation study

The photocatalytic degradation of the Ni-doped ZnO/GO nanocomposites were evaluated using methylene blue (MB) dye on each interval under direct sunlight irradiation as shown in Figure 1. In a typical procedure, 10 mg of photocatalyst was dispersed in 100 mL of 10 mg/L of MB aqueous solution for every run. Prior to irradiation, the suspension was magnetically stirred for 30 min under dark condition to reach the adsorption/desorption equilibrium. Following that, the suspensions were subsequently exposed to sunlight irradiation under continuous stirring for 120 min. At predetermined time intervals, an aliquot of 5 mL of sample was extracted out and the residual concentration was monitored using UV-vis spectrophotometer at λ_{max} = 664 nm. The percentage of degradation of MB was calculated using equation (1). All the photocatalytic degradation experiments were carried out under similar condition on a sunny day from 12.00 to 2 pm, in the month of Mac where the temperature was T= (34±2) ºC at Bandar Tun Abdul Razak Jengka, Pahang.

$$\text{Percentage of degradation (\%)} = (C_o - C_t)/C_o * 100 \quad (1)$$

where C_0 is the concentration of MB before irradiation, while C_t is the concentration of MB at time 't'.

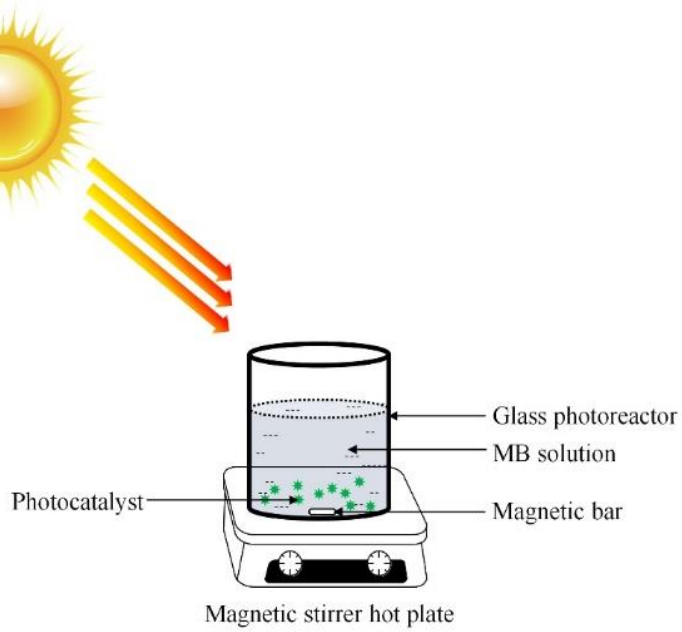

Figure 1. Illustration of the degradation process of Ni-doped ZnO/GO nanocomposites against MB under sunlight irradiation

Results and Discussion

X-ray diffraction pattern analysis

The crystalline phases of the pure and nanocomposites samples were analyzed by XRD, and the corresponding diffraction patterns are shown in Figure 2. Typically, all the diffraction peaks of pure ZnO (Figure 2a) are indexed according to the standard reference of hexagonal ZnO wurtzite structure (JCPDS No. 36-1451). The diffraction peaks at 2θ of 31.8°, 34.4°, 36.4°, 47.6°, 62.9°, 66.6°, 67.9° and 69.2° were respectively

assigned to the (100), (002), (101), (102), (103), (112) and (201), and were consistent with hexagonal zincite structure of pure ZnO [25, 26].

Meanwhile, Figure 2b shows the pattern for the peak of Ni obtained at 44.59° and 51.97° that corresponded to the (111) and (200) crystal faces of Ni standard pattern (JCPDS No. 04-0850) [27]. GO powder exhibits a diffraction peak at 26° corresponding to the (002) plane as can be seen in Fig. 2c. Interestingly, the presence of ZnO wurtzite structure with a very small peak of Ni were identified in the Ni-doped ZnO sample (Figure 2d). The existing of small Ni peak might be due to very small doping content of Ni element. All samples of Ni-doped ZnO/GO displayed the characteristic peaks belonging to ZnO (Figure 2e–h). However, the characteristic peak of Ni and GO was not observed in the XRD patterns possibly because of the low Ni and GO content (0.1 to 0.4 g), which is below the detection range of the XRD instrument. Also, no shift was observed in the position of ZnO diffraction peaks as compared to pure ZnO, proving that the native crystalline structure of ZnO had been maintained after the preparation of the hybrid heterostructure materials. The XRD analysis also revealed that the Ni and GO were incorporated into the wurtzite structure of ZnO crystal as there was no impurity or secondary phases existed in the pattern for all Ni-doped ZnO/GO samples.

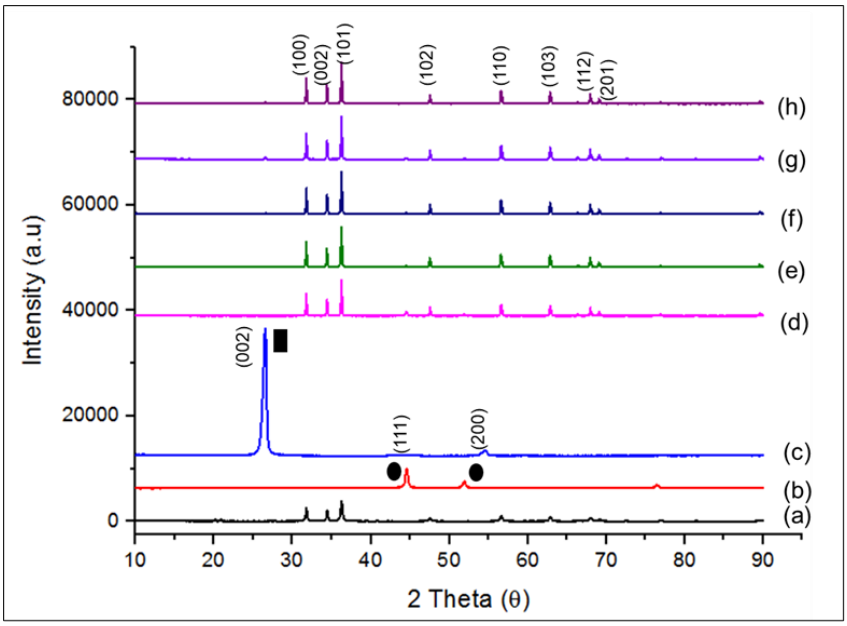

Figure 2. X-ray diffraction patterns of (a) pure ZnO, (b) pure Ni, (c) GO, (d) Ni-doped ZnO, and (e-h) Ni-doped $ZnO/GO_{0.1-0.4}$. (GO and Ni labelled as black square and circle in the graph respectively)

Surface morphological and structural analysis

The surface morphological and structural of pure ZnO, Ni-doped ZnO and Ni-doped $ZnO/GO_{0.1-0.4}$ nanocomposites were characterized by FESEM analysis (Figure 3). It could clearly be seen that similar structure particles with average size of about 100–500 nm was observed for pure ZnO, Ni-doped ZnO and Ni-doped $ZnO/GO_{0.1-0.4}$ nanocomposites. The incorporation of nickel and GO were not visible in the FESEM images. Nonetheless, the overall shapes for all samples composed of rod-like and cubic-like structures.

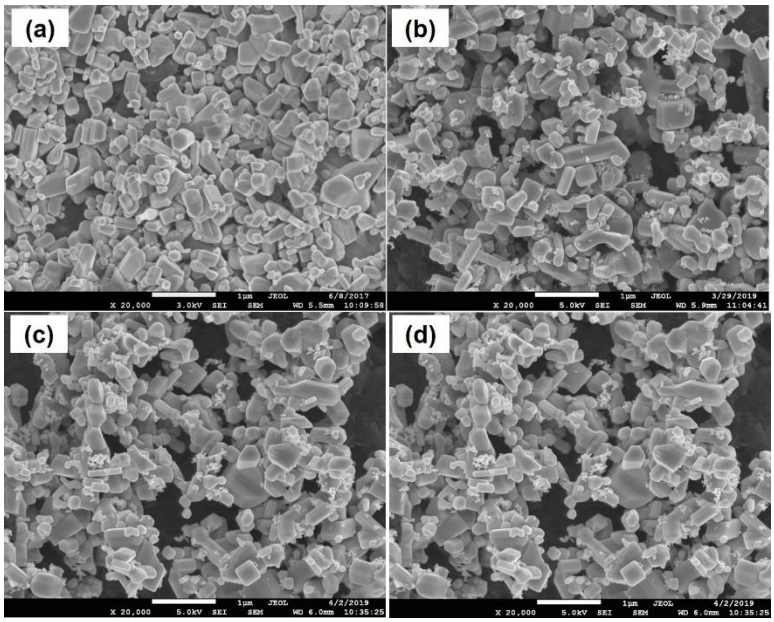

Figure 3. Selected FESEM images for (a) pure ZnO, (b) Ni-doped ZnO, (c) Ni-doped ZnO/$GO_{0.1}$, and (d) Ni-doped ZnO/$GO_{0.4}$

Evaluation of photocatalytic activity

Photocatalytic measurement of Ni-doped ZnO/GO nanocomposites photocatalyst in the removal of MB based on UV-vis spectra is depicted in Figure 4. The overall results revealed that the maximum absorption of MB at 664 nm decreased gradually as a function of time in the presence of different photocatalysts.

All the degradation behaviours were analysed and extrapolated in the following graph as presented in Figure 5. As depicted in the insert of Figure 5, no change was observed in the first 30 min before being exposed to sunlight for photodegradation of MB using ZnO/Ni/$GO_{0.1}$ catalyst because the MB was adsorbed on the surface of catalyst which led to an unchanged concentration and this unable the degradation of MB under dark condition. The photolysis of MB also seems negligible, indicating the stability of MB under sunlight. This is supported from our previous findings where the photolysis of MB under UV light was also insignificant even though UV contains high photon energy (shorter wavelength) as compared to sunlight (longer wavelength) [28]. The photocatalytic activity of pure ZnO reached almost 80% percentage of degradation against MB in aqueous phase. In contrast, the addition of Ni onto the ZnO surface did not improve the degradation efficiency since the percentage obtained was reduced to 15%. The addition of small amount of Ni to the ZnO might contribute to the decreasing of the percentage of degradation. Some researchers had found that the existence of Ni acted as a co-catalyst that reduced the over-potential of electrons at conduction band of ZnO which gave negative effect by lowering the degradation efficiency of ZnO itself. Previously, it was reported that there is high tendency for the occurrence of NiO (as a secondary phase) alongside Ni/ZnO on the catalyst surface which might impose undesirable defects and hence acted as a barrier to light absorption [29]. The transitions of metal ions substituted into the ZnO lattice also act as a recombination centre for electron-hole pairs and subsequently, producing lower percentage of degradation [30]. However, the incorporation of GO (0.1 g) into the samples shows a significant change in photocatalytic activity as compared to pure ZnO and Ni-doped ZnO samples with percentage obtained was around 95%. This was ascribed to the increase in the active sites and enhanced electron mobility which was responsible for the MB degradation.

The photocatalytic enhancement is also attributed by the strong and synergistic interaction between Ni/ZnO and GO in which the GO itself acts as an electron trapping site. The active sites here is referring to the GO surfaces which contain oxygenated functional groups (such as C=O, OH, etc.) that help in enhancing the electron mobility. Graphene itself is known to have superior charge carrier mobility properties (2×10^5 cm^2 V^{-1} s^{-1}) which allow for better electron transfer [31]. Theoretically, when ZnO is receiving the photon energy, the electrons (e^-) excited from the valence band (VB) to the conduction band (CB), leaving positive holes (h^+) behind. These excited electrons are then migrated to the Ni atom and GO sheet and subsequently avoiding the recombination behaviour through effective separation of electron-hole pairs. In this view, more charge carriers are produced from series of redox reactions with subsequent reactive oxidative species (such as •OH and $•O_2^-$) for efficient MB degradation [31]. The recombination could not be avoided if the electrons fall back to the valence band and no photocatalytic reaction could be observed. Thus, an appropriate amount of GO played a crucial role to facilitate the electron transfer and to support ZnO for effective electron mobility and separation of photogenerated charges. The percentage of degradation however decreased significantly at a higher GO content (0.2–0.4 g) due to the agglomeration of the nanocomposites which reduced the surface area and light absorption capacity of the photocatalysts. The percentage obtained for those nanocomposites with varied concentrations of GO displayed were almost comparable to each other.

Even though GO serves as an electron acceptor and mediator for an efficient carrier mobility [32], the presented results also suggested that, different GO content that was incorporated to the Ni-doped ZnO samples significantly affected the degradation efficiency. It might be due to the hindrance of actives sites by excess molecules that simultaneously prevented the light to reach and maximumly absorb the number of dye molecules on the photocatalyst surface. The light scattering and low penetration of light towards the catalyst surface decreased the effective irradiation for the reaction to progress [33]. This phenomenon further reduced the generation of photoexcited electron-hole pairs which leads to the decreased in the photocatalytic performances. This statement is in a good agreement with You et al. in which the decrease in the photocatalytic performance might be due to an excessive presence of GO content which resulted in agglomeration of particles. Hence, the photodegradation rate became more saturated. Furthermore, the higher content of GO in the catalyst lattice could cause a "shielding effect" that might shade the light and limited the light absorption capacity of the photocatalyst [34].

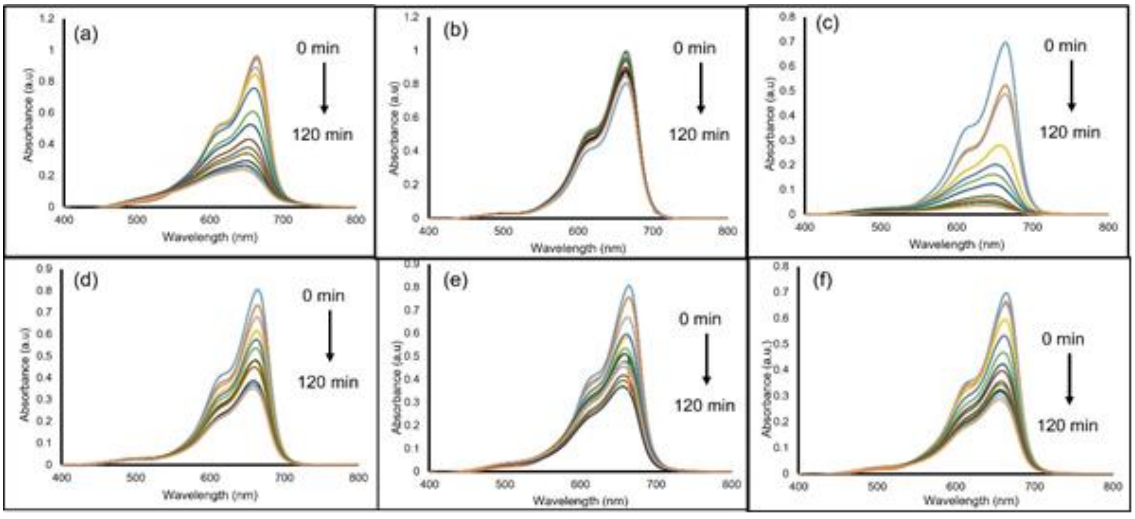

Figure 4. UV–vis absorbance spectra as a function of time for the degradation of MB using (a) pure ZnO, (b) Ni-doped ZnO, and (c – f) Ni-doped ZnO/$GO_{0.1–0.4}$ nanocomposites

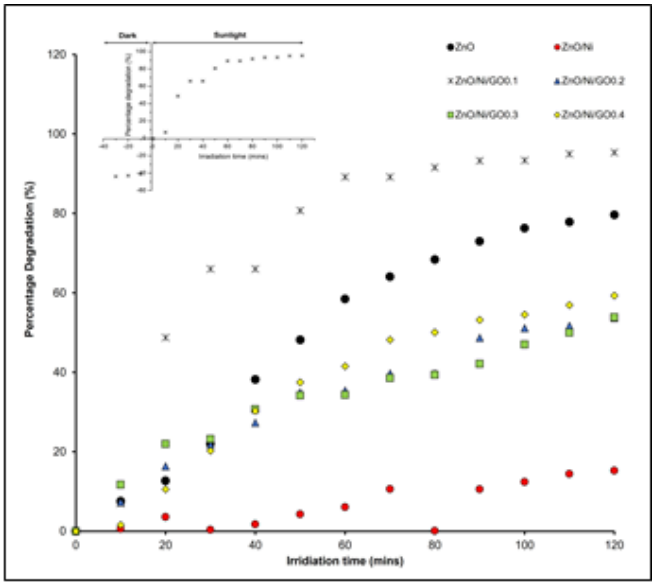

Figure 5. Percentage of degradation of MB under sunlight irradiation in the presence of different photocatalysts and the insert shows the photodegradation of MB under dark and sunlight irradiation using ZnO/Ni/$GO_{0.1}$ catalyst

Further analysis on the kinetic of MB disappearance had been carried out by plotting a first order decay plot of the characteristic of MB absorption peak. The experimental data were fitted based on the Langmuir–Hinshelwood (L–H) kinetic model as expressed by equations (2) and (3), hence the rate constant, *k* of the photocatalyst can be evaluated and quantified.

$$r = dC/dt = kC \quad (2)$$

where *r* and *k* represent the pseudo first-order reaction rate and rate constant, respectively. The equation can be rewritten as

$$\ln (C/C_o) = -kt \quad (3)$$

The pseudo first-order rate constant was determined from the slope of the plot of -ln (Co/Ct) versus irradiation time, t as illustrated in Figure 6. Linear plots were observed (with R^2 values higher than 0.9) which attested that photodegradation of MB obeyed pseudo-first order kinetics. The calculated pseudo-first order rate constant and corresponding R^2 values are presented in Table 1.

The results showed that the Ni-doped ZnO/$GO_{0.1}$ exhibited the highest *k* value of 0.025 min^{-1} compared to other samples which were found to be 0.0138, 0.0013, 0.070, 0.066 and 0.0081 min^{-1} for pure ZnO, Ni-doped ZnO, Ni-doped ZnO/$GO_{0.2}$, Ni-doped ZnO/$GO_{0.3}$, and Ni-doped ZnO/$GO_{0.4}$, respectively. As depicted in Table 1, the incorporation of GO into the Ni-doped ZnO composite influenced the photocatalytic performance as ZnO/Ni/$GO_{0.1}$ nanocomposite exhibited the highest percentage degradation of MB under direct sunlight. It can be suggested that Ni-doped ZnO/$GO_{0.1}$ should be regarded as the best photocatalyst as compared to pure ZnO and other samples. Nevertheless, the incorporation of excess amount of GO to ZnO did not give a significant trend of photodegradation performance due to the hindrance of actives sites by excess molecules that simultaneously prevents the light to reach and maximumly absorbed on the photocatalyst surface. The light scattering and low penetration of light towards the catalyst surface decreasing the effective irradiation for the reaction to progress [9].

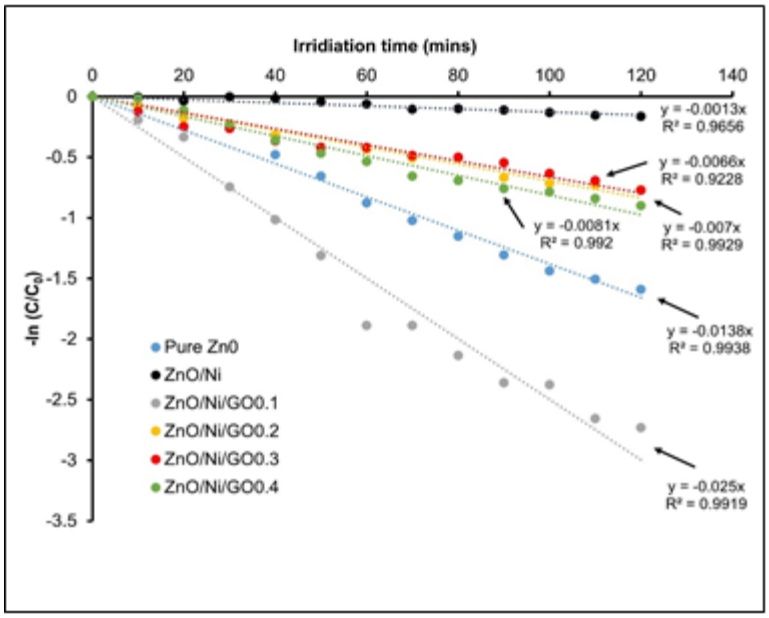

Figure 6. Plots of -ln (C/Co) versus irradiation time for the kinetic of disappearance of MB in the presence of different photocatalysts

Table 1. Photodegradation activities of MB using pure ZnO, Ni-doped ZnO, and Ni-doped ZnO/GO nanocomposites at different GO contents under sunlight irradiation

Sample	Percentage Degradation (%)	Photodegradation Rate Constant, k (min^{-1})	R^2 Value
Pure ZnO	79.64	0.0138	0.9808
ZnO/Ni	15.24	0.0013	0.9102
$ZnO/Ni/GO_{0.1}$	95.33	0.0250	0.9705
$ZnO/Ni/GO_{0.2}$	53.68	0.0070	0.9710
$ZnO/Ni/GO_{0.3}$	53.83	0.0066	0.9228
$ZnO/Ni/GO_{0.4}$	59.32	0.0081	0.9717

Conclusion

In this study, the XRD analysis revealed that the Ni and GO were successfully incorporated into the wurtzite structure of ZnO crystal as there were no impurity or secondary phases existed in the XRD pattern for sample Ni-doped $ZnO/GO_{0.1–0.4}$ nanocomposites. Other than that, it also showed the absence of Ni peak in the nanocomposite samples and this might be due to very small doping content of Ni element. The FESEM images with average size of about 100–500 nm was observed for pure ZnO, Ni-doped ZnO, Ni-doped $ZnO/GO_{0.1}$ and Ni-doped $ZnO/GO_{0.4}$ nanocomposites. Moreover, the morphological characteristics for all prepared samples composed of rod-like and cubic-like structures. The Ni-doped $ZnO/GO_{0.1}$ nanocomposite exhibited the best photocatalytic degradation of MB under direct sunlight within 120 min of reaction with percentage of degradation reaching 93.49% and photodegradation rate constant, k value of 0.0250 min^{-1} as compared to other samples. Overall, this research suggests a viable method

for improving the photocatalytic activity of ZnO-based photocatalysts, and it has promising implications for environmental issues.

Acknowledgement

This research is supported by FRGS-RACER: 600-RMI/FRGS/RACER 5/3 (041/2019). The authors fully acknowledged Ministry of Higher Education (MOHE) and Universiti Teknologi MARA Pahang for the approved fund which makes this important research viable and effective.

References

1. Jeyasubramanian, K., Hikku, G. S. and Sharma, R. K. (2015). Photo-catalytic degradation of methyl violet dye using zinc oxide nano particles prepared by a novel precipitation method and its anti-bacterial activities. *Journal of Water Process Engineering*, 8: 35-44.
2. Subbaiah, M. V. and Kim, D. S. (2016). Adsorption of methyl orange from aqueous solution by aminated pumpkin seed powder: Kinetics, isotherms, and thermodynamic studies. *Ecotoxicology and environmental safety*, 128:109-117.
3. Peter, A., Mihaly-Cozmuta, A., Nicula, C., Mihaly-Cozmuta, L., Jastrzębska, A., Olszyna, A. and Baia, L. (2017). UV light-assisted degradation of methyl orange, methylene blue, phenol, salicylic acid, and rhodamine B: photolysis versus photocatalyis. *Water, Air, & Soil Pollution*, 228(1): 1-12.
4. Kheirabadi, M., Samadi, M., Asadian, E., Zhou, Y., Dong, C., Zhang, J. and Moshfegh, A. Z. (2019). Well-designed Ag/ZnO/3D graphene structure for dye removal: Adsorption, photocatalysis and physical separation capabilities. *Journal of Colloid and Interface Science*, 537: 66-78.
5. Jothibas, M., Manoharan, C., Jeyakumar, S. J., Praveen, P., Punithavathy, I. K. and Richard, J. P. (2018). Synthesis and enhanced photocatalytic property of Ni doped ZnS nanoparticles. *Solar Energy*, 159: 434-443.
6. Rafaie, H. A., Nor, R. M., Azmina, M. S., Ramli, N. I. T. and Mohamed, R. (2017). Decoration of ZnO microstructures with Ag nanoparticles enhanced the catalytic photodegradation of methylene blue dye. *Journal of Environmental Chemical Engineering*, *5*(4): 3963-3972.
7. Syazwani, O. N., Mohd Hir, Z. A., Mukhair, H., Mastuli, M. S. and Abdullah, A. H. (2019). Designing visible-light-driven photocatalyst of Ag_3PO_4/CeO_2 for enhanced photocatalytic activity under low light irradiation. *Journal of Materials Science: Materials in Electronics*, 30(1): 415-423.
8. Asghar, A., Raman, A. A. A. and Daud, W. M. A. W. (2015). Advanced oxidation processes for in-situ production of hydrogen peroxide/hydroxyl radical for textile wastewater treatment: a review. *Journal of Cleaner Production*, 87: 826-838.
9. Mohd Hir, Z. A., Abdullah, A. H., Zainal, Z. and Lim, H. N. (2017). Photoactive hybrid film photocatalyst of polyethersulfone-ZnO for the degradation of methyl orange dye: Kinetic study and operational parameters. *Catalysts*, 7(11): 313.
10. Khaki, M. R. D., Shafeeyan, M. S., Raman, A. A. A. and Daud, W. M. A. W. (2017). Application of doped photocatalysts for organic pollutant degradation-A review. *Journal of Environmental Management*, 198: 78-94.
11. Bora, L. V. and Mewada, R. K. (2017). Visible/solar light active photocatalysts for organic effluent treatment: Fundamentals, mechanisms and parametric review. *Renewable and Sustainable Energy Reviews,* 76: 1393-1421.
12. Ahmed, S. N. and Haider, W. (2018). Heterogeneous photocatalysis and its potential applications in water and wastewater treatment: a review. *Nanotechnology,* 29(34): 342001.
13. Wang, P., Wu, D., Ao, Y., Wang, C. and Hou, J. (2016). ZnO nanorod arrays co-loaded with Au nanoparticles and reduced graphene oxide: Synthesis, characterization and photocatalytic application. *Colloids and Surfaces A: Physicochemical and Engineering Aspects,* 492: 71-78.

14. Zhu, P., Duan, M., Wang, R., Xu, J., Zou, P. and Jia, H. (2020). Facile synthesis of ZnO/GO/Ag_3PO_4 heterojunction photocatalyst with excellent photodegradation activity for tetracycline hydrochloride under visible light. *Colloids and Surfaces A: Physicochemical and Engineering Aspects,* 602: 125118.
15. Upadhyay, G. K., Rajput, J. K., Pathak, T. K., Kumar, V. and Purohit, L. P. (2019). Synthesis of ZnO: TiO_2 nanocomposites for photocatalyst application in visible light. *Vacuum,* 160: 154-163.
16. Muñoz-Fernandez, L., Sierra-Fernández, A., Milošević, O. and Rabanal, M. E. (2016). Solvothermal synthesis of Ag/ZnO and Pt/ZnO nanocomposites and comparison of their photocatalytic behaviors on dyes degradation. *Advanced Powder Technology,* 27(3): 983-993.
17. Xie, M., Zhang, D., Wang, Y. and Zhao, Y. (2020). Facile fabrication of ZnO nanorods modified with RGO for enhanced photodecomposition of dyes. *Colloids and Surfaces A: Physicochemical and Engineering Aspects,* 603: 125247.
18. Wang, W., Li, N., Hong, K., Guo, H., Ding, R. and Xia, Z. (2019). Z-scheme recyclable photocatalysts based on flower-like nickel zinc ferrite nanoparticles/ZnO nanorods: enhanced activity under UV and visible irradiation. *Journal of Alloys and Compounds*, 777: 1108-1114.
19. Tawale, J. S., Kumar, A., Swati, G., Haranath, D., Dhoble, S. J. and Srivastava, A. K. (2018). Microstructural evolution and photoluminescence performanance of nickel and chromium doped ZnO nanostructures. *Materials Chemistry and Physics*, 205: 9-15.
20. Gao, P., Ng, K. and Sun, D. D. (2013). Sulfonated graphene oxide–ZnO–Ag photocatalyst for fast photodegradation and disinfection under visible light. *Journal of Hazardous Materials,* 262: 826-835.
21. Ahmad, M., Ahmed, E., Hong, Z. L., Khalid, N. R., Ahmed, W. and Elhissi, A. (2013). Graphene–Ag/ZnO nanocomposites as high performance photocatalysts under visible light irradiation. *Journal of Alloys and Compounds,* 577: 717-727.
22. Haghshenas, S. S. P., Nemati, A., Simchi, A. and Kim, C. U. (2019). Dispute in photocatalytic and photoluminescence behavior in ZnO/graphene oxide core-shell nanoparticles. *Materials Letters,* 240: 117-120.
23. Moussa, H., Girot, E., Mozet, K., Alem, H., Medjahdi, G. and Schneider, R. (2016). ZnO rods/reduced graphene oxide composites prepared via a solvothermal reaction for efficient sunlight-driven photocatalysis. *Applied Catalysis B: Environmental,* 185: 11-21.
24. Wu, Z. and Wang, L. (2019). Graphene oxide (GO) doping hexagonal flower-like ZnO as potential enhancer of photocatalytic ability. *Materials Letters,* 234: 287-290.
25. Długosz, O., Szostak, K., Krupiński, M. and Banach, M. (2021). Synthesis of Fe_3O_4/ZnO nanoparticles and their application for the photodegradation of anionic and cationic dyes. *International Journal of Environmental Science and Technology,* 18(3): 561-574.
26. Huszla, K., Wysokowski, M., Zgoła-Grześkowiak, A., Staszak, M., Janczarek, M., Jesionowski, T. and Wyrwas, B. (2022). UV-light photocatalytic degradation of non-ionic surfactants using ZnO nanoparticles. *International Journal of Environmental Science and Technology,* 19(1): 173-188.
27. Li, J., Li, P., Li, J., Tian, Z. and Yu, F. (2019). Highly-dispersed Ni-NiO nanoparticles anchored on an SiO_2 support for an enhanced CO methanation performance. *Catalysts,* 9(6): 506.
28. Rafaie, H. A., Embong, N. A., Ramli, N. I., Mohamed, R. and Kasim, M. F. (2018). Synthesis of ZnO microstructure decorated with ag nanoparticles at different annealing temperature and their photocatalytic activity. *Recent Innovations in Chemical Engineering (Formerly Recent Patents on Chemical Engineering)*, 11(3): 192-200.
29. Behnood, R. and Sodeifian, G. (2020). Synthesis of N doped-CQDs/Ni doped-ZnO nanocomposites for visible light photodegradation of organic pollutants. *Journal of Environmental Chemical Engineering,* 8(4), 103821.

30. Yin, Q., Qiao, R., Li, Z., Zhang, X. L. and Zhu, L. (2015). Hierarchical nanostructures of nickel-doped zinc oxide: Morphology controlled synthesis and enhanced visible-light photocatalytic activity. *Journal of Alloys and Compounds,* 618: 318-325.
31. Julkapli, N. M. and Bagheri, S. (2015). Graphene supported heterogeneous catalysts: an overview. *International Journal of Hydrogen Energy,* 40(2): 948-979.
32. Ahmad, M., Ahmed, E., Ahmed, W., Elhissi, A., Hong, Z. L. and Khalid, N. R. (2014). Enhancing visible light responsive photocatalytic activity by decorating Mn-doped ZnO nanoparticles on graphene. *Ceramics International,* 40(7): 10085-10097.
33. Qin, J., Zhang, X., Xue, Y., Kittiwattanothai, N., Kongsittikul, P., Rodthongkum, N. and Liu, R. (2014). A facile synthesis of nanorods of ZnO/graphene oxide composites with enhanced photocatalytic activity. *Applied Surface Science,* 321: 226-232.
34. Tju, H., Shabrany, H., Taufik, A. and Saleh, R. (2017). Degradation of methylene blue (MB) using ZnO/CeO2/nanographene platelets (NGP) photocatalyst: Effect of various concentration of NGP. In *AIP Conference Proceedings,* 1862: p. 030037.